**Research article**

Ivan Shutsko, Christian Michael Böttge, Jonas von Bargen, Andreas Henkel, Maik Meudt and Patrick Görrn*

# Enhanced hybrid optics by growing silver nanoparticles at local intensity hot spots

**Abstract:** Silver nanoparticles (AgNPs) show an extraordinary strong interaction with light, which enables confinement and field enhancement at the nanoscale. However, despite their localized nature, such phenomena are often sought to be exploited on a larger device length scale, for example, in sensors, solar cells, or photocatalytic cells. Unfortunately, this is often limited by strong absorption. One way to reduce these losses is to first focus light with low loss dielectric optics and then to place the AgNPs in that focus. Here, we present a clear experimental proof that growth of AgNPs from the liquid phase at a substrate surface can be controlled by light. Violet light of 405 nm and 1.5 W/cm$^2$ is coupled into thin film resonators and locally focused at their surface. The AgNPs grow at the focus position with sub-Abbe alignment accuracy. Numerical simulations confirm that this alignment causes an increased field enhancement within the AgNPs and is therefore expected to lead to an improved performance of the resulting hybrid devices.

## 1 Introduction

Hybrid optics is an emerging field enabling to combine the benefits of high localization with the benefits of low loss

propagation. Dielectric optical systems are often characterized by long-range propagation yielding high-quality resonators [1, 2]. On the other hand, plasmonics enables strong confinement of light at the nanoscale. A combination of both in one hybrid device can be highly beneficial.

One example visualizing such benefits is shown in Figure 1. Silver nanoparticles placed on a dielectric substrate and directly illuminated show sub-Abbe confinement and consequently field enhancement. This is depicted in red in Figure 1F, indicating the absolute value of the electric field strength on the surface of a dielectric substrate and the corresponding cross section in Figure 1B. By placing the AgNPs on top of a thin film resonator (Figure 1C and F, black curve), at the places where the evanescent tails of the standing wave have maximum electric field strength, this phenomenon can be strongly enhanced (Figure 1D and F, blue curve) as the light interacting with the AgNPs can be collected on a larger area. However, once the particles show only a slight misplacement, the benefit is lost (Figure 1E and F, green curve). In fact, the local field strength in case of misalignment is even lower than for the pure AgNPs on the dielectric substrate (Figure 1B and red curve in Figure 1F).

This example in Figure 1 shows the importance of alignment of plasmonic nanoparticles in respect to the thin film resonator. Such an aligned hybrid device in Figure 1D, where plasmonic nanoparticles are placed on the exact positions of maximum interaction with a thin film resonator, will allow to locally confine an incoming electromagnetic radiation harvested from a much larger area. At the same time, it emphasizes the technological challenge related to hybrid optics to produce such devices in a cost-efficient way (Figure 1A).

In particular, exact positioning of the plasmonic nanoparticles at the correct places of thin film resonators or other focusing optical elements like lenses or tapered waveguides will not only increase local field strength, but also often results in higher efficiency of hybrid devices. It also reduces the demand of rare and expensive coinable metals required for nanoscale confinement of visible light

**\*Corresponding author: Patrick Görrn,** University of Wuppertal, School of Electrical, Information and Media Engineering, Chair of Large Area Optoelectronics, Wuppertal, North Rhine-Westphalia, Germany, e-mail: goerrn@uni-wuppertal.de
**Ivan Shutsko, Christian Michael Böttge, Jonas von Bargen, Andreas Henkel and Maik Meudt:** University of Wuppertal, School of Electrical, Information and Media Engineering, Chair of Large Area Optoelectronics, Wuppertal, North Rhine-Westphalia, Germany. https://orcid.org/0000-0002-3788-0318 (I. Shutsko)
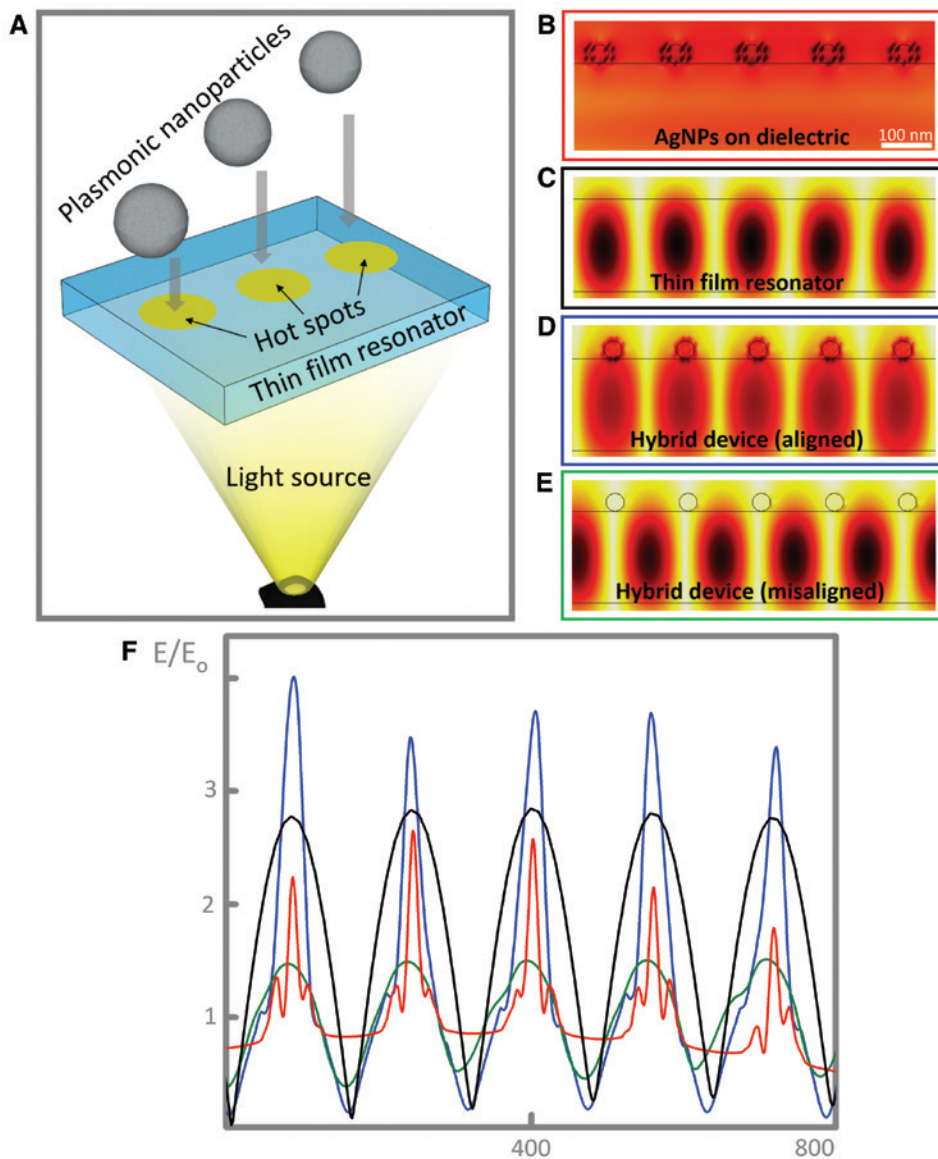
**Figure 1:** The benefit of maximized interaction between the plasmonic nanoparticles and thin film resonator in a hybrid device. (A) Schematic illustration of the challenge related to hybrid optics in positioning of plasmonic nanoparticles at the hot spots of a large-area thin film resonator. (B) 20 nm AgNPs placed on a dielectric substrate. (C) Standing electromagnetic wave inside the thin film resonator. (D) 20 nm AgNPs placed on the thin film resonator at the maximum of evanescent field strength. (E) 20 nm AgNPs placed on the thin film resonator and shifted to the positions of minimum evanescent field strength. (F) Electric field strength on the surface of the dielectric with AgNPs on top (red curve), thin film resonator without AgNPs (black curve), aligned (blue curve) and misaligned (green curve) hybrid device.

within large-scale optoelectronic devices. It is especially desirable for the production of solar cells [3] or sensors [4–7] and displays [8], where cost is of critical importance. For the growing field of water splitting devices [9–11] based on excitation of localized surface plasmon resonance (LSPR) under solar radiation, this approach would also further reduce the amount of photocatalyst needed [12]. However, accurate optimum positioning of plasmonic nanoparticles cannot be handled by state-of-the-art

technology. In this paper, we have addressed that challenge illustrated in Figure 1A.

The interaction of waveguide modes with plasmonic nanostructures is studied by many research groups in the field of hybrid optics. In recent studies [13–17], the focus was put on the investigation of coupling between dielectric waveguide modes with plasmonically active nanoparticles such as silver or gold nanoparticles (AgNPs or AuNPs), placed on top of a waveguide to explore the optical properties of

a hybrid device. In such hybrid devices, nanoparticles are excited through an evanescent tail of a propagating dielectric waveguide mode. Depending on the waveguide geometry and the morphology of the metallic nanoparticles, this coupling leads to a fascinating modification of an optical response of the waveguide through resonant scattering and absorption on NPs [13, 14], outcoupling through NPs [15], strong coupling regime [16], or energy transfer from guided modes into plasmonic waveguide modes [17].

Methods, influencing the growth of AgNPs, usually rely on the mechanical or chemical preparation of the substrate [18–31]. Hence, the substrate positions must be known, and the preparation often requires expensive techniques such as electron beam or focused ion beam lithography. On the other hand, nanoparticle trapping allows to control the positions of AgNPs with optical intensity gradients [32]. Unfortunately, only AgNPs that are already grown to their maximum size can be influenced this way as the needed intensity strongly increases with lower particle diameter. Another drawback is the fact that the optical forces exist under light exposure only and vary with the power of the incident light. In order to fix the particles, they must be welded to the subjacent film using even higher intensities, which further limits the applicability of nanoparticle trapping [33].

Nowadays, well-known bottom-up colloidal methods allow producing sophisticated nanoparticles with perfect control at the atomic scale [34–38]. On the other hand, using top-down approaches [37–39], the precise positioning and interparticle spacing could be reached [40, 41]. However, a technique for bottom-up growing nanoparticles at the desired places within a hybrid device has not been proposed.

In this paper, we will demonstrate a novel technique for the fabrication of a hybrid device with maximized interaction between plasmonic nanoparticles and large-scale thin film resonator. We will show how to grow AgNPs from liquid phase at the exact places of maximum intensity. Such hot spots on the thin film resonator are formed at a resonance condition. We utilize the absorption of light to start the growth mechanism from the atomic scale. As a consequence, small light intensities can be applied and AgNPs are permanently fixed even at touchy films. We chose a thin film resonator produced by transfer printing and spin-coating to demonstrate the general use of our approach.

## 2 Materials and methods

The experiments were divided into three parts: preparation of a thin film resonator, AgNP growth on top, and characterization of the obtained nanopattern. First, the silver stripes with gaps of around 200 nm width were fabricated using a shadowing effect during thermal evaporation of silver at a certain angle onto the PDMS (polydimethylsiloxan) blazed grating. Afterward, the stripes were transfer printed onto a glass substrate [42]. A polystyrene film spin-coated on top was flattened mechanically in order to ensure that the surface relief is not influenced by the underlying silver gaps (supporting information, Figure S3A, B).

The width of the gaps between the metal stripes and the quality of the flattened polystyrene were characterized by an atomic force microscope. A detailed description of the sample preparation procedure can be found in the supporting information.

The second part of the experiment was the electroless growth of the AgNPs on top of the polystyrene film from the liquid phase (ELD solution). The employed silver solution was prepared in accordance with [43] and was slightly modified in order to increase the light sensitivity (50 drops of 6 v/v % ammonia solution were added additionally). The supporting information provides more details on electroless AgNP growth.

In the end, the ELD solution was cast on the polystyrene film and illuminated from the bottom glass side with a CW laser with the wavelength of 405 nm and a power density of about 1.5 W/cm². After 1 min of illumination, the drop of ELD solution was removed by nitrogen flow. The resulting distribution of nanoparticles was analyzed with a scanning electron microscope and an atomic force microscope (see supporting information).

## 3 Results and discussion

As thin film resonator, we used a stack of a glass substrate ($n_g = 1.47$), silver stripes with 200 nm gaps and a period of 1.66 µm, and a polymer film on top ($n_p = 1.62$). Details about the preparation are described in the methods above and Supporting Information of this article (sections "Blazed angle evaporation and transfer printing" and "Flattening of polymer film"). By illuminating the thin film resonator (Figure 2A) from the glass bottom side with a plane wave in TM polarization, surface plasmons are excited propagating on both interfaces of the silver film from the gap. On the other hand, by choosing TE polarization, TE dielectric modes are excited at the gaps and coupled into the polymer film. This way, the presented structure of the thin film resonator is able to support both delocalized surface plasmon waves and dielectric modes.
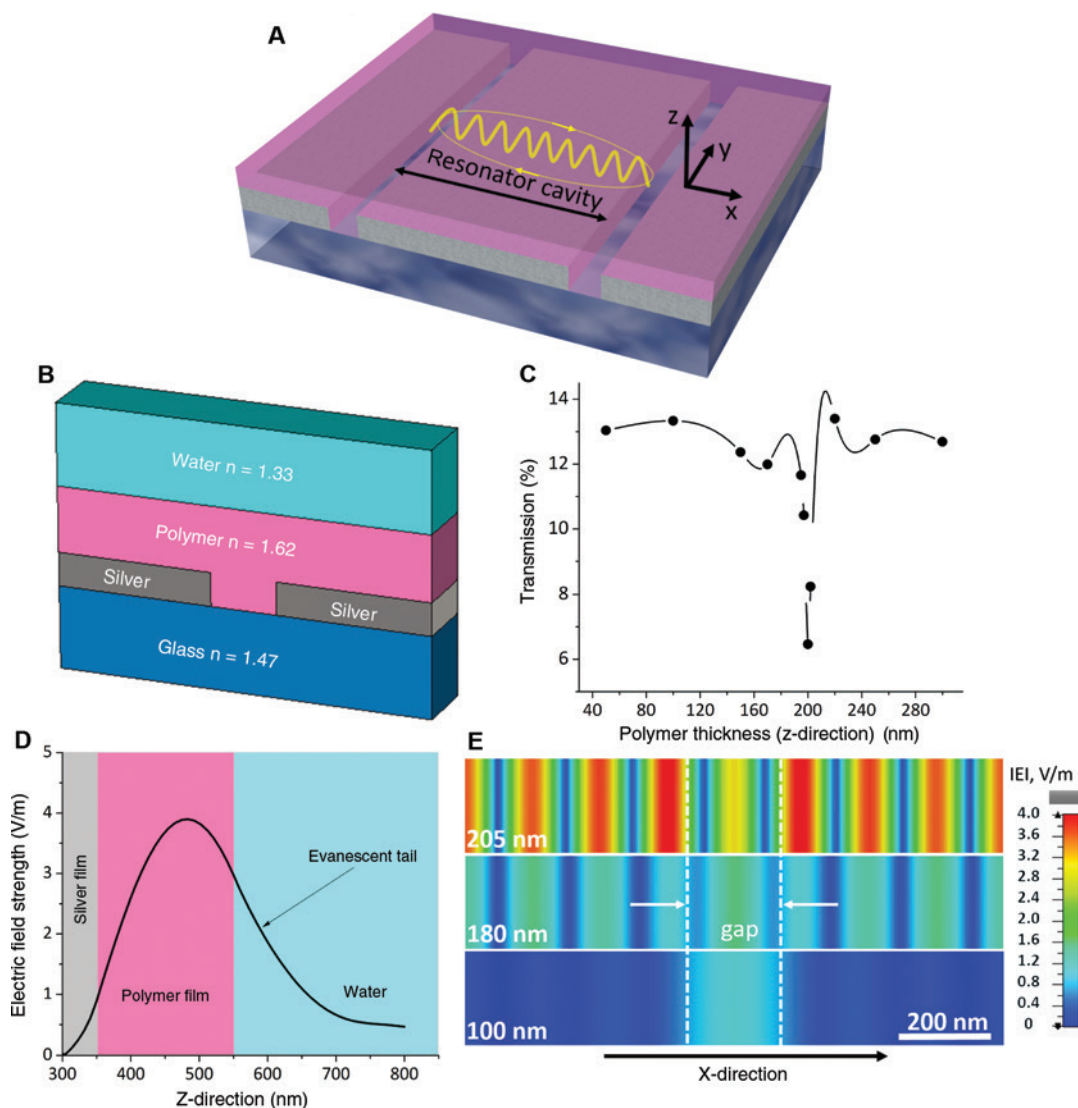
**Figure 2:** Simulation of thin film resonator.
(A) Schematic illustration of the resonator cavity in polymer film. (B) Thin film resonator structure with water mimicking the ELD solution. (C)Transmission of TE-polarized light (405 nm) through the thin film resonator at different thicknesses of the polymer film. (D) Evanescent wave of the resonator mode. (E) 2D cut of absolute value of electric field strength distribution on the polymer film surface at its thicknesses of 205, 180, and 100 nm (view from the surface side of the thin film resonator), the white dashed line indicates the area with a gap between silver stripes.

In this work, we have focused on the resonant excitation of TE dielectric modes in the polymer film.

To analyze the optical properties of the resonator, a numerical simulation (time and frequency domain solver of CST Studio Suite) is applied. The simulated structure is covered with water mimicking the ELD solution (electroless deposition) needed for AgNP growth (Figure 2B). When the thin film resonator is illuminated with a TE-polarized plane wave at the wavelength of 405 nm, around 12–14% of the light is transmitted through, depending on the thickness of the polymer film (Figure 2C). At a thickness of the polymer film of around 205 nm, the transmission drops,

because incident light is coupled into TE modes and guided inside the polymer film forming a mode resonance. The resonance is lost as soon as there is only a slight change of the thickness of the polymer film, which can also be seen in the sharp drop of transmission in Figure 2C. The simulations show that the resonance is also very sensitive to variations of the gap width, even by a few percent.

The evanescent wave of the resonator mode in Figure 2D shows pronounced tails decaying over about 130 nm into the water (direction z). Accordingly, the electric field strength in the evanescent tail in water is three times higher than in an incident plane wave. The

evanescent wave amplitude varies harmonically with the distance from the gap (direction x, Figure 2E). By decreasing the thickness of the polymer film, the resonance is lost and the corresponding strength of electric field in evanescent tails drop dramatically. The evanescent wave on the surface of polymer film at the thicknesses of 180 and 100 nm is compared with a thickness of 205 nm (Figure 2E). The maxima of the plotted absolute values of electric field strength in the evanescent waves in Figure 2E show a distance of 145 nm. Therefore, it can be concluded that the wavelength of the film mode is 290 nm. This value is in good agreement with the wavelength of the wave propagating in the polymer film between silver and water with an effective refractive index of 1.39, calculated using the transfer matrix method.

The harmonically varying evanescent wave formed on the surface of the thin film resonator serves as a driver for the nucleus formation and further plasmon-mediated growth of AgNPs [44] from ELD solution. The proposed model of the growth mechanism of AgNPs on the surface of polystyrene is described in detail in the supporting information. It has been demonstrated before that the arrangement of AgNPs grown in a similar way but without focus is influenced by the parameters of the light source [43]. That has been interpreted as a growth mechanism mediated by local intensity variations. However, a direct control of the AgNP positions utilizing this phenomenon has not yet been reported.

To prove the idea that growth takes place at hot spots on the polymer film surface where the evanescent wave has the maximum value of electric field strength, the ELD solution is cast on top of the 180 nm polymer film of the thin film resonator, which is kept under a CW laser irradiation in TE polarization (Figure 3A). The scanning electron micrograph of the obtained nanopattern after 1 min

of illumination is shown in Figure 3B. It confirms that growth of AgNPs was mediated at the places of maximum evanescent field strength (Figure 2E).

The 2D nanopattern consists of two types of lines: thick lines with a period of 1.66 μm formed of coalescing AgNPs above the gaps (see Figure 2A and dashed white lines in Figure 2E) and thin lines between, with a period of around 145 nm. The width of the thick lines corresponds to the width of the gap (around 200 nm). The thin lines consist of AgNPs with an average diameter of around 40 nm. The period of the lines is 145 nm, which corresponds to half of the wavelength of the simulated evanescent wave on the surface of the polymer film $\lambda_0/(2 \times n_{eff})$, see Figure 2E. This feature size also defines the resolution limit usually found in light-induced patterning. The fact that the lines are clearly distinguishable confirms sub-Abbe positioning accuracy of the AgNPs, which is explained by LSPR excitation. The number of the lines matches the simulated number of maxima shown in Figure 2E. For a better illustration of areas with thick and thin AgNP lines, we have marked them out with different colors and performed a fast Fourier transform analysis of the highlighted areas with thin lines to determine the period of the lines (see supporting information).

The AgNP growth rate above the gaps is higher than for the particles between the gaps (Figure 3B). This observation is in agreement with the simulation results in Figure 2E for the polymer film with 180 nm of thickness, where the evanescent field strength above the gap is higher than throughout the entire surface area between the gaps. As it was predicted by the simulation, thickness variation of the polymer film has a strong impact on the resonance behavior of our prepared structure. The thickness measurements show a deviation of 25 nm from the desired thickness of 205 nm.
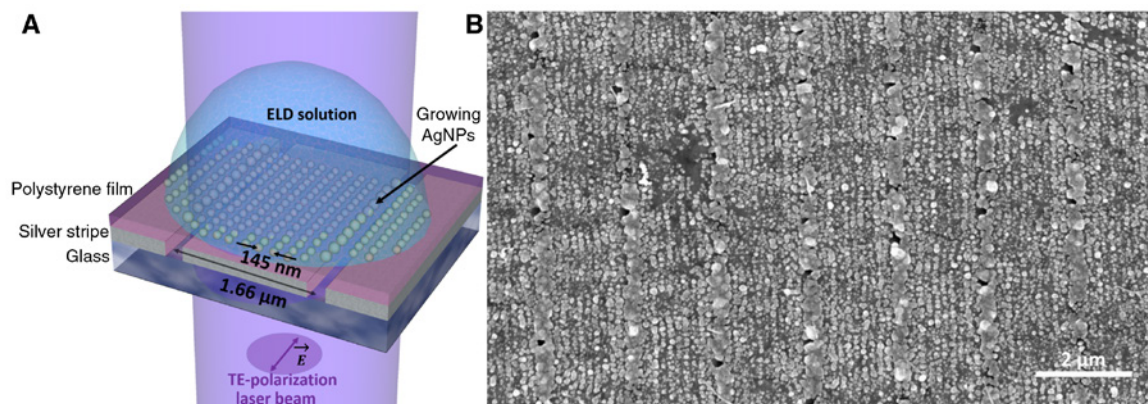


**Figure 3:** Experimental creation of the optimized hybrid device by growing AgNPs at the local intensity hot spots of the thin film resonator. (A) Schematic illustration of AgNP growth on top of the 180 nm polystyrene film of the thin film resonator. (B) Scanning electron micrographs of the AgNPs on the polystyrene.

Even such small thickness variations of ±10% cause significant changes in the simulated field distribution as emphasized in Figure 2E.

To check the adhesion between grown AgNPs and the polystyrene film, the structure was treated with a supersonic bath at room temperature. After 10 min, we observed the partial removal of the particles from the places between the gaps. After 15 min, the thin lines were almost removed, whereas the thick lines above the gaps remained almost unchanged (see morphology development at the SEM micrographs in the supporting information, Figure S6). This experiment supports our idea that light exposure locally increases the adhesion of AgNPs on the substrate [45, 46] through plasmon-mediated photooxidation, and adhesion increases with the intensity of the light confined at a hot spot.

According to Figure 1, the alignment of AgNPs at the positions of maximum intensity should also lead to their increased interaction with the incident light wave. While Figure 1 used a simplified resonator geometry, we now probe the resonance behavior of the experimentally realized hybrid device consisting of the thin film resonator with the AgNPs on top through numerical simulations of the near- and far-field optical properties. It is found that the simulated hybrid device with AgNPs at the positions of maximum interaction with the thin film resonator shows

efficient confinement of the incoming light for the AgNPs with a diameter corresponding to LSPR. At the same time, a small shift from the right position leads to strongly decreased coupling between modes of thin film resonator and AgNPs, which is shown in Figure S7A, B, C in the supporting information. Moreover, by examining a scattering cross section we observed a significant modification of the far-field scattering directions when AgNPs are shifted to the optimized positions (Figure S7D).

The parameters enhanced in our hybrid device, absorption and scattering, depend not only on the alignment of AgNPs on the hot spots but also on the shape and size of the AgNPs. For instance, the size of the AgNPs grown with the presented method is optimal for increased interaction with the incident laser beam. Therefore, the increased absorption and scattering cannot be unambiguously attributed to alignment using these devices. In order to experimentally prove the impact of alignment, more selective parameters would be helpful. That is why the decision was in favor of a different device, hybrid waveguide couplers. These show a more direct interaction between two waves via interference, a mechanism that relies on the interplay of many AgNPs, and thus on alignment. These experimental results can be found in the supporting information (section "Hybrid waveguide couplers by optimized alignment of AgNPs").
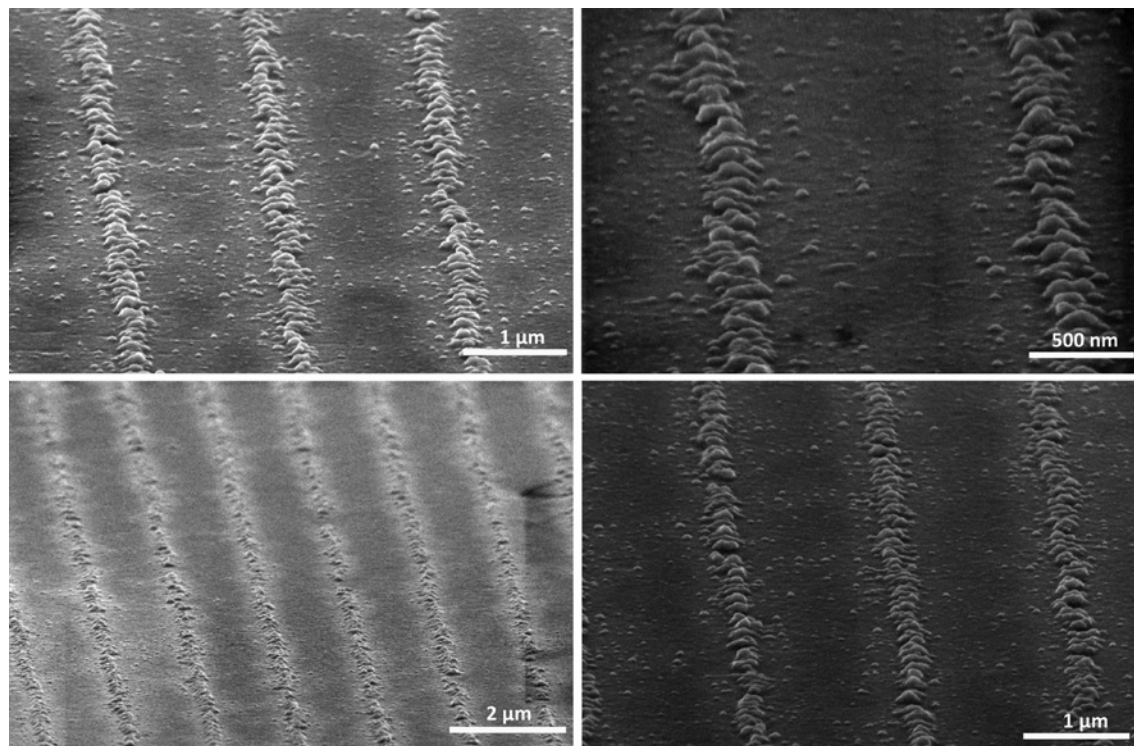


**Figure 4:** Scanning electron micrographs of AgNPs on 100 nm polystyrene film growing above the gaps.

In our second set of experiments, we aimed to suppress resonator TE modes in the polymer film by decreasing the thickness from 180 to 100 nm where these waves can be neglected (Figure 2E). In this case, the resulting electric field on top of the polymer film is found above the gaps. As predicted by the simulation in that case, we observed an alignment of the AgNPs on the surface of the polymer above the gaps only (Figure 4). No growth between the gaps is observed. This result also confirms that AgNP growth between the gaps requires dielectric modes forming hot spots at the resonator (compare the case of 180 and 100 nm polymer thickness in Figure 2E).

The nanopatterning is observed on the entire area of the laser spot (2 mm). The width of the grown lines varies between 200 and 220 nm, which corresponds to the simulation of the near-field distribution on the dielectric surface above the gap. The diameter of the nanoparticles stays in the range of 50–60 nm and could be varied by the used wavelength [43, 44, 47]. Furthermore, in our case, we observe a slight coalescence of nanoparticles, which can be controlled by time and the concentration of silver ions in the solution [48]. The surface tension has an impact on the shape of the formed nanoparticle. The more hydrophobic the surface, the more the shape becomes spherical. Here, the shape is explained by a low surface energy of the polystyrene film (52 mN/m).

## 4 Conclusion

In summary, we have shown that AgNPs are grown at local intensity focus spots. These spots were created with a thin film resonator produced by spin-coating and transfer printing. Such facile scalable focusing structures could improve the efficiency of plasmon phenomena in low cost or even large area applications and, at the same time, reduce the amount of plasmon or photocatalyst material needed. However, usually with increasing focus, e.g., increasing quality factor, the sensitivity toward imperfections is also increased. In fact, in many practical cases, variations of the exact focus positions will have to be accepted. This is where we anticipate the benefit of our method compared with other top-down methods. As the light of the focusing device directly controls the AgNP growth, it automatically enforces the creation of an optimized hybrid system.

## References

[1] Poon JKS. Integrated ultra-low-loss resonator on a chip. Nat Photon 2018;12:255–6.

[2] Cai DP, Lu JH, Chen CC, Lee CC, Lin CE, Yen TJ. High Q-factor microring resonator wrapped by the curved waveguide. Sci Rep 2015;5:10078.

[3] Alwater HA, Polman A. Plasmonics for improved photovoltaic devices. Nat Mater 2010;9:205–13.

[4] Peyskens F, Wuytens P, Raza A, Van Dorpe P, Baets R. Waveguide excitation and collection of surface-enhanced Raman scattering from a single plasmonic antenna. Nanophotonics 2018;7:1299–306.

[5] Wang H, Li H, Xu S, Zhao B, Xu W. Integrated plasmon-enhanced Raman scattering (iPERS) spectroscopy. Sci Rep 2017;7:14630.

[6] Cortés E, Xie W, Cambiasso J, et al. Plasmonic hot electron transport drives nano-localized chemistry. Nat Commun 2017;8:14880.

[7] Sánchez-González A, Corni S, Mennucci B. Surface-enhanced fluorescence within a metal nanoparticle array: the role of solvent and plasmon couplings. J Phys Chem C 2011;115:5450–60.

[8] Hsu CW, Zhen B, Qiu W, et al. Transparent displays enabled by resonant nanoparticle scattering. Nat Commun 2014;5:3152.

[9] Xiao FX, Liu B. Plasmon-dictated photo-electrochemical water splitting for solar-to-chemical energy conversion: current status and future perspectives. Adv Mater Interfaces 2018;5:1701098.

[10] Warren SC, Thimsen E. Plasmonic solar water splitting. Energ Environ Sci 2012;5:5133–46.

[11] Lee J, Mubeen S, Ji X, Stucky GD, Moskovits M. Plasmonic photoanodes for solar water splitting with visible light. Nano Lett 2012;12:5014–9.

[12] Wei Q, Wu S, Sun Y. Quantum-sized metal catalysts for hot-electron-driven chemical transformation. Adv Mater 2018;30:1802082.

[13] Stuart HR, Hall DG. Enhanced dipole-dipole interaction between elementary radiators near a surface. Phys Rev Lett 1998;80:5663.

[14] Quidant R, Girard C, Weeber JC, Dereux A. Tailoring the transmittance of integrated optical waveguides with short metallic nanoparticle chains. Phys Rev B 2004;69:085407.

[15] Arango FB, Kwadrin A, Koenderink FA. Plasmonic antennas hybridized with dielectric waveguides. ACS Nano 2012;6:10156–67.

[16] Magno G, Fevrier M, Gogol P, et al. Strong coupling and vortexes assisted slow light in plasmonic chain-SOI waveguide systems. Sci Rep 2017;7:7228.

[17] Février M, Gogol P, Aassime A, et al. Giant coupling effect between metal nanoparticle chain and optical waveguide. Nano Lett 2012;12:1032–7.

[18] Baraldi G, Bakhti S, Liu Z, et al. Polarization-driven self-organization of silver nanoparticles in 1D and 2D subwavelength gratings for plasmonic photocatalysis. Nanotechnology 2017;28:035302.

[19] Liu Z, Destouches N, Vitrant G, et al. Understanding the growth mechanisms of Ag nanoparticles controlled by plasmon-induced charge transfers in Ag-TiO2 films. J Phys Chem C 2015;119:9496–505.

[20] Eurenius L, Hägglund C, Olsson E, Kasemo B, Chakarov D. Grating formation by metal-nanoparticle-mediated coupling of light into waveguided modes. Nat Photon 2008;2:360–4.

[21] Goutaland F, Colombier J-P, Sow MC, Ollier N, Vocanson F. Laser-induced periodic alignment of Ag nanoparticles in soda-lime glass. Opt Express 2013;21:31789–99.

[22] Wisser FM, Schumm B, Mondin G, Grothe J, Kaskelab S. Precursor strategies for metallic nano- and micropatterns using soft lithography. J Mater Chem C 2015;3:2717–31.

[23] Gangopadhyay AK, Krishna H, Favazza C, Miller C, Kalyanaraman R. Heterogeneous nucleation of amorphous alloys on catalytic nanoparticles to produce 2D patterned nanocrystal arrays. Nanotechnology 2007;18:485606.

[24] Pang Z, Zhang X. Direct writing of large-area plasmonic photonic crystals using single-shot interference ablation. Nanotechnology 2011;22:145303.

[25] Kuznetsov AI, Evlyukhin AB, Gonçalves MR, et al. Laser fabrication of large-scale nanoparticle arrays for sensing applications. ACS Nano 2011;5:4843–9.

[26] Peláez RJ, Baraldi G, Afonso CN, Riedel S, Boneberg J, Leiderer P. Selective gold nanoparticles formation by pulsed laser interference. Appl Surf Sci 2011;258:9223–7.

[27] Kaempfe M, Graener H, Kiesow A, Heilmann A. Formation of metal particle nanowires induced by ultrashort laser pulses. Appl Phys Lett 2001;79:1876–8.

[28] Kiesow A, Strohkark S, Löschner K, et al. Generation of wavelength-dependent, periodic line pattern in metal nanoparticle-containing polymer films by femtosecond laser irradiation. Appl Phys Lett 2005;86:153111.

[29] Loeschner K, Seifert G, Heilmann A. Self-organized, grating like nanostructures in polymer films with embedded metal nanoparticles induced by femtosecond laser irradiation. J Appl Phys 2010;108:073114.

[30] Bagratashvili VN, Rybaltovskii AO, Ilyukhin SS, et al. Laser-induced growth and self-organization of silver nanoparticles in colloidal polymers. Las Phys 2014;24:126001.

[31] Meudt M, Jakob T, Polywka A, et al. Metasurfaces: plasmonic black metasurface by transfer printing. Adv Mater Technol 2018;3:1800124.

[32] Bosanac L, Aabo T, Bendix PM, Oddershede LB. Efficient optical trapping and visualization of silver nanoparticles. Nano Lett 2008;8:1486–91.

[33] Maragò OM, Jones PH, Gucciardi PG, Volpe G, Ferrari AC. Optical trapping and manipulation of nanostructures. Nat Nanotechnol 2013;8:807–19.

[34] Zhang Q, Li W, Moran C, et al. Seed-mediated synthesis of Ag nanocubes with controllable edge lengths in the range of

[35] Wiley BJ, Wang Z, Wei J, Yin Y, Cobden DH, Xia Y. Synthesis and electrical characterization of silver nanobeams. Nano Lett 2006;6:2273–8.

[36] Xia Y, Xiong Y, Lim B, Skrabalak SE. Shape-controlled synthesis of metal nanocrystals: simple chemistry meets complex physics? Angew Chem Int Ed 2009;48:60–103.

[37] Pelton M, Aizpurua J, Bryant G. Metal-nanoparticle plasmonics. Lasd Photon Rev 2008;2:136–59.

[38] Wiley B, Sun Y, Xia Y. Synthesis of silver nanostructures with controlled shapes and properties. Acc Chem Res 2007;40:1067–76.

[39] Gurevich EL, Gurevich SV. Laser Induced Periodic Surface Structures induced by surface plasmons coupled via roughness. Appl Surf Sci 2014;30:118–23.

[40] Henzie J, Lee MH, Odom TW. Multiscale patterning of plasmonic metamaterials. Nat Nanotechnol 2007;2:549–54.

[41] Merkel TJ, Herlihy KP, Nunes J, Orgel RM, Rolland JP, DeSimone JM. Scalable, shape-specific, top-down fabrication methods for the synthesis of engineered colloidal particles. Langmuir 2010;26:13086–96.

[42] Jakob T, Polywka A, Stegers L, et al. Transfer printing of electrodes for organic devices: nanoscale versus macroscale continuity. Appl Phys A 2015;120:503–8.

[43] Polywka A, Tückmantel C, Görrn P. Light controlled assembly of silver nanoparticles. Sci Rep 2017;7:45144.

[44] Langille MR, Personick ML, Mirkin CA. Plasmon-mediated syntheses of metallic nanostructures. Angew Chem Int Edn 2013;52:13910–40.

[45] Polywka A, Vereshchaeva A, Riedl T, Görrn P. Manipulating the morphology of silver nanoparticles with local plasmon-mediated control. Part Part Syst Charact 2014;31:342–6.

[46] Tanabe I, Tatsuma T. Plasmonic manipulation of color and morphology of single silver nanospheres. Nano Lett 2012;12:5418–21.

[47] Callegari A, Tonti D, Chergui M. Photochemically grown silver nanoparticles with wavelength-controlled size and shape. Nano Lett 2003;3:1565–8.

[48] José-Yacamán M, Gutierrez-Wing C, Miki M, Yang DQ, Piyakis KN, Sacher E. Surface diffusion and coalescence of mobile metal nanoparticles. J Phys Chem B 2005;109:9703–11.